Transgenic Activation of Ras in Neurons Promotes Hypertrophy and Protects from Lesion-induced Degeneration

Rolf Heumann,* Christoph Goemans,* Daniela Bartsch,* Kurt Lingenhöhl,§ Peter C. Waldmeier,§ Bastian Hengerer,§ Peter R. Allegrini,§ Karl Schellander, Erwin F. Wagner,‖ Thomas Arendt,¶ Rigobert H. Kamdem,¶ Kirstin Obst-Pernberg,‡ Frank Narz,* Petra Wahle,‡ and Hartmut Berns***

*Ruhr-University of Bochum, Molecular Neurobiochemistry and ‡Developmental Neurobiology, D-44780 Bochum, Germany; §Novartis, CH-4002 Basel, Switzerland; ‖Research Institute of Molecular Pathology (IMP), A-1030 Vienna, Austria; ¶Paul-Flechsig-Instititute for Brain Research, D-04109 Leipzig, Germany; and **University of Bonn, Institute of Animal Breeding Science, D-53115 Bonn, Germany

Abstract. Ras is a universal eukaryotic intracellular protein integrating extracellular signals from multiple receptor types. To investigate its role in the adult central nervous system, constitutively activated V12-Ha-Ras was expressed selectively in neurons of transgenic mice via a synapsin promoter. Ras-transgene protein expression increased postnatally, reaching a four- to fivefold elevation at day 40 and persisting at this level, thereafter. Neuronal Ras was constitutively active and a corresponding activating phosphorylation of mitogen-activated kinase was observed, but there were no changes in the activity of phosphoinositide 3-kinase, the phosphorylation of its target kinase Akt/PKB, or expression of the anti-apoptotic proteins Bcl-2 or Bcl-X_L. Neuronal Ras activation did not alter the total number of neurons, but induced cell soma hypertrophy, which resulted in a 14.5% increase of total brain volume. Choline acetyltransferase and tyrosine hydroxylase activities were increased, as well as neuropeptide Y expression. Degeneration of motorneurons was completely prevented after facial nerve lesion in Ras-transgenic mice. Furthermore, neurotoxin-induced degeneration of dopaminergic substantia nigra neurons and their striatal projections was greatly attenuated. Thus, the Ras signaling pathway mimics neurotrophic effects and triggers neuroprotective mechanisms in adult mice. Neuronal Ras activation might become a tool to stabilize donor neurons for neural transplantation and to protect neuronal populations in neurodegenerative diseases.

Key words: Ras • neuron • transgenic • protection • mouse

Introduction

The Ras/mitogen-activated protein kinase (MAPK)[1] (extracellular signal–regulated kinase [ERK]) pathway is an evolutionary conserved signaling pathway found in all eukaryotic cells, including yeast (Marshall, 1996). In mammals, the Ras family comprises Ha-Ras, Ki-Ras, and N-Ras that are all lipid-anchored proteins in the inner face of membranes, cycling between the inactive GDP-bound and the signaling competent GTP-bound conformation. A network of upstream mechanisms converge onto the activation of Ras by using distinct types of Ras GTPase activating proteins (GAPs) or Ras-guanine nucleotide exchange factors (Wittinghofer, 1998) that respond to extracellular ligand–receptor triggered signaling cascades and intracellular second messengers (Reuther and Der, 2000). The mammalian RAS-guanine nucleotide exchange factor son of sevenless (mSOS1,2) is activated by receptor tyrosine kinases, whereas the guanine nucleotide release factors (Ras-GRF1,2) and the guanine nucleotide release protein are involved in calcium channel–mediated or G-protein–coupled receptor mechanisms. Conversely, a family of distinct types of Ras-GAP proteins regulate GTP hydrolysis: besides 120Ras-GAP and GAP1, neurofibromin (NF)-1, a protein that is deficient in patients with von Reckling-

F. Narz, P. Wahle, and H. Berns contributed equally to this work.

Address correspondence to Rolf Heumann, Ruhr-University of Bochum, Molecular Neurobiochemistry, NC/7-174, 44870 Bochum, Germany. Tel.: 49-23-43-22-42-30. Fax: 49-23-43-21-41-05. E-mail: rolf.heumann@ruhr-uni-bochum.de

H. Berns' present address is University of Basel, Department of Clinical-Biological Sciences (DKBW) and Research, Hebelstr. 20, CH-4031 Basel, Switzerland.

[1]*Abbreviations used in this paper:* Chat, choline acetyltransferase; ERK, extracellular signal–regulated kinase; GAD, glutamic acid decarboxylase; GAP, GTPase activating protein; IRES, internal ribosomal entry site; lacZ, β-galactosidase; MAPK, mitogen-activated protein kinase; MPP^+, 1-methyl-4-phenylpyridinium; MPTP, *N*-methyl-4-phenyl-1,2,3,6-tetrahydropyridine; NF, neurofibromin; NMR, nuclear magnetic resonance; NPY, neuropeptide Y; P, postnatal; PI 3-kinase, phosphoinositide 3-kinase; PKB, phosphoinositide-dependent protein kinase; TG, transgene; TH, tyrosine hydroxylase; wt, wild-type; 6-OHDA, 6-hydroxydopamine.

hausen disease type 1, is regulated by lipids (Bollag and McCormick, 1991; Lockyer et al., 1999). The brain-specific synGAP is negatively regulated by intracellular calcium concentrations (Kennedy, 1998).

In cultured neural cells, the intracellular functions of Ras strictly depend on the cell type investigated: in transformed astrocytes proliferation depends on Ras (Guha et al., 1997), yet in nerve growth factor responsive–PC12 pheochromocytoma tumor cells, Ras has been shown to stop proliferation and induce neurite outgrowth (Bar-Sagi and Feramisco, 1985; Noda et al., 1985). Moreover, neuronal survival has been demonstrated to depend on Ras, as shown by the intracellular application of function blocking anti-Ras F_{ab} fragments into cultured embryonic neurons in vitro (Borasio et al., 1993) or inactive Ras (N17 Ras) (Xue et al., 2000). Consistently, cultured neurotrophin-deprived embryonic neurons derived from dorsal root ganglia, superior cervical ganglion, nodose ganglia, ciliary ganglia, or spinal cord are rescued from apoptosis by the intracellular application of activated Ras protein or cDNA (Borasio et al., 1989; Nobes et al., 1996; Weng et al., 1996; Xue et al., 2000)

How can Ras activation direct specific downstream functions in neurons? The major pathways induced by Ras are Raf-1/B-raf/MAPK, Ral-GDS/phospholipase D/Rho, and phosphoinositide 3-kinase (PI 3-kinase)/Akt-1(phosphoinositide-dependent protein kinase [PKB]) (Katz and McCormick, 1997). The latter signaling branch has been shown to promote survival in many neuronal systems (Williams and Doherty, 1999). In addition to PI 3-kinase, MAPK (ERK) activation is necessary for neuronal survival, but this pathway may regulate distinct apoptotic signaling cascades (Xue et al., 2000). In cultured cerebellar neurons, MAPK (ERK) activates the ribosomal Rsk-kinase, which, in turn, phosphorylates and thereby inactivates the proapoptotic activity of Bad (Bonni et al., 1999). The latter belongs to the Bcl-2 family of apoptosis-regulating proteins, forming homotypic or heterotypic dimers.

An in vivo function of Ras in the intact nervous system has been implicated from genetically induced deficiencies: expression of a dominant-negative mutant of c-Raf increased apoptosis during early development of the retina (Pimentel et al., 2000). Furthermore, inactivation of the neuronal-specific Ras-guanine nucleotide release factor 1 in mice resulted in an impairment of long-term potentiation in the amygdala (Brambilla et al., 1997). Conversely, mice deficient in Ha-Ras showed an enhanced long-term potentiation at the CA1 Schaffer colaterals of the hippocampus (Manabe et al., 2000). In NF-1 gene knock-out mice, spatial learning deficiencies are found (Silva et al., 1997), and in patients suffering from von Recklinghausen disease type 1, cognitive functions are impaired. Interestingly, nuclear magnetic resonance (NMR) measurements showed that in these patients the brain volume is increased probably due to a relative change in grey matter volume (Moore et al., 2000). Although the mechanism of this brain expansion is not known, it has been suggested that NF deficiency results in delayed apoptosis. Indeed, cultured peripheral neurons from mouse embryos with a targeted disruption of the NF-1 gene are able to survive in the absence of neurotrophic supply (Vogel et al., 1995).

However, the general applicability of the concept of Ras-mediated neuronal survival has been challenged because, in contrast to superior cervical ganglion neurons, NGF-mediated survival of sympathetic chain neurons is completely uncoupled from Ras activity (Borasio et al., 1993; Markus et al., 1997). Here, we expressed constitutively activated Ha-Ras selectively in neurons by using the neuronal promoter for the synapsin I gene, allowing us to directly investigate the effects of enhanced Ras activity on neuronal survival postnatally. Moreover, we asked if neuronal Ras activation could mimic typical neurotrophic effects, such as neuronal hypertrophy, induction of neuropeptide Y (NPY), or increase in neurotransmitter synthesizing enzyme activities.

Materials and Methods

Establishment of the Transgene and Transgenic Mouse Lines

The 5′ nontranslated regions of the human *Ha-Ras* (Capon et al., 1983) and the rat *Synapsin I* (Sauerwald et al., 1990) genes were fused. The 3′ flanking region of the *Ha-Ras* gene, including its polyadenylation signal, was removed and substituted with a fragment containing internal ribosomal entry site (*IRES)/LacZ* (Kalnins et al., 1983; Ghattas et al., 1991). A linear 10.1-kb DNA fragment, without vector sequences, was recovered and was suitable for mouse embryo manipulation.

Pronucleus DNA injections and embryo transfers were carried out according to standard procedures. 15-μg DNA from tail biopsies of each progeny aged 3 wk were restricted with KpnI, separated on 1.1% agarose gels, blotted to nylon membranes, and hybridized to a radioactively labeled *Ras* probe. Detected 1.9-kb DNA fragments represented 1.6 kb of the *Synapsin I* promoter and 0.3 kb of the *Ha-Ras* gene at their connection point, indicating transgene specificity. Outbred lines $B6CBF_1$, $B6CBF_1xMF_1$, and $HimOF_1xMF_1$ were used as embryo donors and recipients. Founders were further bred with lines $HimOF_1$, C57BL/6 (Institute for Animal Breeding and Genetics, University of Veterinary Medicine, Vienna, Austria), and NMRI (Central Institute for Laboratory Animal Breeding, Hannover, Germany).

Lines 46 and 50 were crossed back to NMRI background. They contained one integration site each with multiple transgene integrants. Whereas line 46 was bred to homozygocity, putative homozygous animals of line 50 could not be obtained. Ras-transgenic mice (syn Ras-TG) of lines 46 and 50 developed normally and did not show obvious behavioral differences to wild-type (wt) littermates.

Western Blots

Tissue was lysed in ice-cold lysis buffer (50 mM Tris-HCl, pH 7.4, 150 mM NaCl, 40 mM NaF, 5 mM EDTA, 5 mM EGTA, 1% [vol/vol] NP-40, 0.1% sodiumdesoxycholate, 0.1% SDS, 10 μg/ml aprotinin, 1 mM PMFS) using a 1-ml Dounce homogenizer. After centrifugation (13,000 *g*, 15 min, 4°C), the supernatants were collected. The protein concentration was determined using the DC protein assay (Bio-Rad Laboratories). Equal amounts of protein were separated on 12% polyacrylamide gels, as described by Laemmli. After blotting to 0.2-μm nitrocellulose (Schleicher & Schuell), the blots were blocked with 5% dry milk in TBST (10 mM Tris-HCl, pH 7.6, 150 mM NaCl, 0.05% Tween 20). The immunoreactive bands were detected using the indicated antibodies, horseradish peroxidase–conjugated secondary antibodies (Sigma-Aldrich) and the enhanced chemiluminescence substrate detection kit (Amersham Pharmacia Biotech). The following primary antibodies were used: anti–Ha-Ras (OP23; Calbiochem), anti–pan-Ras (OP40; Calbiochem), anti–phospho-MAPK (9106S; New England Biolabs), anti–synapsin I, anti–phospho-Akt (9271S; New England Biolabs, Inc.), anti–Bcl-2 (clone 7; Signal Transduction Laboratories); and anti–Bcl-X_L (clone 4; Signal Transduction Laboratories).

Glutathione-S-transferase–Ras-binding Domain Fusion Protein Pulldown Assay and PI 3-kinase Assay

Precipitation of GTP-Ras was performed essentially as described previously (de Rooij and Bos, 1997). For the determination of PI 3-kinase activity, tissues were Dounce homogenized on ice in lysis buffer (1% NP-40, 140 mM NaCl, 20 mM Tris-HCl, 1 mM $MgCl_2$, 1 mM $CaCl_2$, 1 mM Na_3VO_4, 10% glycerol, 1 mM PMSF, 10 μg/ml aprotinin, at pH 7.4). After clearing the lysate by centrifugation, the protein concentration was deter-

mined using the Bio-Rad DC protein assay kit. 400 μg of protein, in a volume of 500 μl, was used for immunoprecipitation with either 10 μg anti-pTyr (PY20; Transduction Laboratories) or 10 μg anti-Ras mAb Y13-259 plus 5 μg anti–rat IgG. The associated PI 3-kinase activity was determined as described previously (Virdee et al., 1999).

Primary Neuronal Cultures

Embryonic brains (embryonic day [E]14) were dissected and the midbrain was transferred to a tube containing $MPBS^{-/+}$ (10 mM Hepes-NaOH, pH 7.4, 137 mM NaCl, 2.7 mM KCl, 8 mM Na_2HPO_4, 1.5 mM KH_2PO_4, 10 mM glucose, 1 mM sodium pyruvate, 1 mg/ml BSA, 2 mM glutamax [Sigma-Aldrich], 6 μg/ml DNase I, 5 μg/ml phenol red, 100 U/ml penicillin, 100 μg/ml streptomycin, 5.8 mM $MgCl_2$). After incubation with trypsin (0.25%, 15 min, 37°C) (GIBCO BRL), the tissue was washed twice with DME/+5 (containing 2 mM glutamax, 10% heat-inactivated fetal calf serum, 100 U/ml penicillin, 100 μg/ml streptomycin, 37.5 μg/ml insulin, 5 mM glucose, 10 mM Hepes-NaOH, pH 7.4, in DME [GIBCO BRL]) and twice with $MPBS^{-/+}$. The tissue was dissociated by using a pipette tip, and seeded to polyornithin-coated 3.5-cm culture dishes with grid (Nunc) containing 1.5 ml DME/+ 5. The cells from one embryo were plated on two dishes. After 24 h, the serum containing DME/+5 was removed, the cells were washed three times with $PBS^{+/+}$ and 1.5 ml of B18 medium (modified from Brewer and Cotman, 1989), and the cells were prepared lacking catalase, reduced glutathione, and superoxide dismutase. Cells were cultured at 37°C in 10% CO_2. Cells were treated either with 150 μM 6-hydroxydopamine (6-OHDA) for 90 min after 6 d in vitro or with 1 μM 1-methyl-4-phenylpyridinium (MPP^+) for 36 h after 4 d in vitro. Dopaminergic neurons were detected using a primary tyrosine hydroxylase (TH) antibody (1017381; Roche Diagnostics), a biotin-conjugated secondary antibody (B8774; Sigma-Aldrich), and extravidin-FITC (Sigma-Aldrich).

TH and Choline Acetyltransferase (Chat) Assay

The TH assay was performed as described (Bostwick and Le, 1991). For the Chat assay, different brain regions were dissected and the tissues were homogenized by sonication in 5 mM Tris-acetate, pH 7.4, and 0.1% Triton X-100 (vol/vol). The lysate was cleared twice by centrifugation, and an aliquot of the supernatant was removed for determination of the protein content. Equal amounts of the lysate were assayed for Chat activity (Fonnum, 1975). The linearity of the enzymatic reactions was verified with different amounts of lysate.

Facial Nerve Axotomy, Histochemistry, Western Blot Analysis, and Facial Motorneuron Plane Determination

Five synRas-TG and five wt littermates, both 10 wk old, were subjected to transection of the right facial nerve. Mice were anesthetized with 1–1.5% isoflurane in a 70:30 nitrous oxide/oxygen (vol/vol) mixture. A nerve segment was removed to avoid contact of the nerve endings. Because cell bodies of motorneurons degenerate very slowly after axonal transection (Kou et al., 1995), mice were analyzed at 24 d after lesion. After cardial perfusion with 4% paraformaldehyde, brains were postfixated, immersed in 30% sucrose, frozen and cut into 20-μm frontal sections, and then followed by Nissl staining of every third section. Facial motorneuron counting of stained sections was performed by nucleolus identification. Plane size determination of 100 facial motorneurons from all the mice per group was performed by image analysis system MCID M4 from Image Research, Inc.

Cortical Volume, Numerical Density, and Number of Cortical Neurons

Cortical volume was calculated from the cortical cross-sectional areas obtained by planimetry on serial coronal sections (final magnification: 50×) throughout the entire length of the cortex. Numerical neuronal density was determined by the dissector method (Sterio, 1984). Measurements were taken on semithin sections (final magnification: 500×) throughout the cortical depth in five randomly located samples of the frontal, parietal, and occipital cortex. The total number of neurons was estimated from the mean numerical neuronal density and the total cortical volume.

Determination of Dopamine after In Vivo MPTP Lesion, as well as in Unlesioned Mice

Eight synRas-TG and eight wt adult littermates were treated twice with 30 mg/kg (subcutaneous) *N*-methyl-4-phenyl-1,2,3,6-tetrahydropyridine (MPTP, obtained as the hydrochloride salt; RBI) at an interval of 72 h. They were killed together with 11 synRas-TG and 10 wt untreated adult littermates by decapitation 21 d after the second MPTP injection. Striata were dissected, weighed, and homogenized (Branson sonifier B12) in 2 ml 0.15 M chloroacetic acid containing 75 mg/liter EDTA and 200 ng/ml α-methyl-dihydroxyphenylalanine, as an internal standard. The homogenate was adjusted to pH 2.9 using 2 N NaOH and centrifuged at 40,000 *g* for 10 min. The supernatants were frozen overnight and recentrifuged before quantification of dopamine by HPLC with electrochemical detection, as described previously (Waldmeier et al., 1993).

In Situ Hybridization and Anatomical and Morphometric Analysis

For in vivo magnetic resonance imaging measurements, five synRas-TG and five wt adult littermates were analyzed on a 4.7 tesla 30-cm bore Bruker DBX (Bruker), according to a published method (Allegrini and Sauer, 1992) adapted for mice.

For histochemical analysis, mice were killed (overdose of Nembutal, 60 mg/kg body weight i.p.) and perfusion-fixed, as described previously (Obst and Wahle, 1995). A surface view of each brain was drawn at 16× final magnification with a camera lucida. To process wt and synRas-TG brains at the same time, the hemispheres were paired, embedded in Tissue Tek, frozen, cut in 30-μm-thick serial sections, and processed for free-floating in situ hybridization, as described previously (Obst and Wahle, 1995; Wahle et al., 2000). For detection of the Ras-TG transcript, a 827-bp region of the lacZ cDNA cloned into pBS SK was used to generate digoxigenin UTP–labeled antisense riboprobes (Roche). Furthermore, riboprobes against glutamic acid decarboxylase (GAD) mRNA and NPY mRNA were employed (Wahle et al., 2000). β-Galactosidase (lacZ) staining of fixed-brain sections (in 2% paraformaldehyde/0.2% glutaraldehyde, 30 min at 4°C) was performed using a 5-bromo-4-chloro-3-indolyl-β-D-galactopyranoside (X-gal)–staining solution. The morphometric analysis was carried out on thionin-stained brain sections of pairs of mice (siblings of one wt and one synRas-Tg) aged postnatal day (P) 13 and 40, as well as 2 and 6 mo. Somata of large pyramidal neurons of neocortical layer V of motor and somatosensory cortex and Purkinje cells of the cerebellum were outlined with a camera lucida at 1,000× magnification. Drawings were digitalized, and a somatic area in square micrometer was determined with an AutoCAD system for at least 150 somata of every population, which were then statistically compared using a nonparametric test. Soma sizes were fed into size-frequency histograms.

Results

Neuronal Expression of Constitutively Active Ras in Neurons Leads to an Increase in Postnatal Cortical Brain Volume Without Affecting Neuronal Cell Number

The synapsin I promoter was used to drive the selective expression of V12-Ha-Ras in postmitotic neurons (Sauerwald et al., 1990; Hoesche et al., 1993; Lietz et al., 1998) and minimize the risk of a deregulated cell number or tumor formation (Sweetser et al., 1997; Holland et al., 2000). The transgene encoded for a dicistronic mRNA, which directs the synthesis of two separate proteins, V12-Ha-Ras and LacZ (Fig. 1 A), and was tested for its Ras activity by transfection and induction of fiber outgrowth in PC12 cells (data not shown).

In the resulting heterozygous syn-Ras-TG mice (line 50), the levels of activated Ha-Ras (Ras-TG) protein were very low in the embryo, as revealed by Western blots (not shown) using antibodies selectively recognizing Ha-Ras, but not N-Ras or Ki-Ras protein. The major increase in V12-Ha-Ras expression occurred postnatally in the cortex of synRas-TG mice, which start to rise at P4, elevate threefold by P13, and reach four- to fivefold basal levels by P40 (Fig. 1 B). In wt littermates, endogenous Ha-Ras increased only moderately during postnatal development. There was

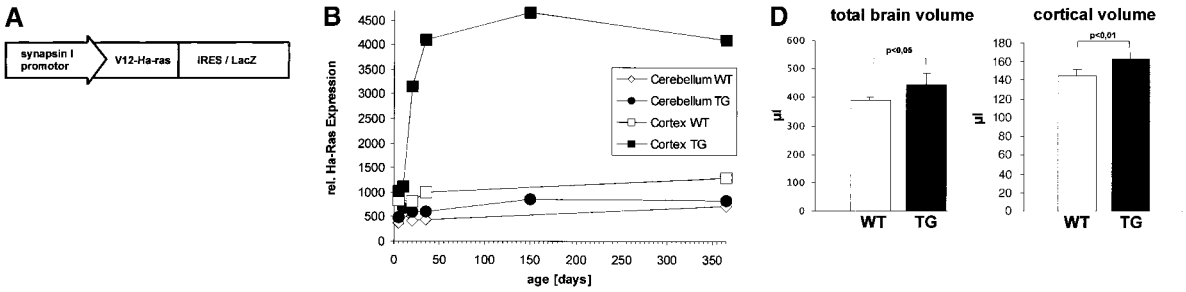

Figure 1. Generation of Ras-transgenic mice: developmental expression of constitutively activated Ras and increased brain volume in adult mice. (A) Schematic diagram of the bicistronic transgene construct. The Ras-TG expression was driven by the neuron-specific promoter of the synapsin I gene. The structural genes of the construct consisted of the gene for constitutively activated *V12-Ha-Ras* and the *lacZ* gene. An "internal ribosomal entry site" (IRES) is located downstream of the *Ras* stop codon. The bicistronic mRNA generated by this construct is terminated at the polyadenylation site of *LacZ*. *Synapsin I* promoter was from *Rattus norvegicus*; *V12-Ha-Ras*, human *Val12–Ha-Ras* oncogene (R. Jaggi, Inselspital Bern, Bern, Switzerland); *IRES* of encephalomyocarditis virus (J.E. Majors, Washington University School of Medicine, St. Louis, MO); *LacZ* was from *Escherichia coli*. (B) Developmental Ha-Ras expression in various brain regions and at different ages of Ras-transgenic (synRas-TG) mice and wt littermates. Homogenates of brain cortices or cerebella derived from synRas-TG mice and wt littermates were analyzed by Western blotting using an antibody recognizing endogeneous and activated transgenic Ha-Ras. Ras-TG expression was hardly detectable prenatally. In the cortex, there was a rapid postnatal increase reaching a 4.2-fold expression of activated Ras-TG, relative to endogeneous Ha-Ras at 40 d. Only moderate postnatal Ha-Ras increases were seen in wt cortex or in cerebella of wt or synRas-TG mice. Data are the means of two independent experiments, as obtained from densitometric measurements. (C) Horizontal sections of paired brain hemispheres derived from wt (left) or synRas-TG (right) mice after fixation and X-gal staining. Note the intense expression of the transgene in the region of neuronal cell somata of the hippocampus and also in the cortex (black arrows). The cortical brain volume is enlarged, leading to a caudal displacement of the cerebellum (compare white arrows). Bar, 1.8 mm. (D) Total brain volume and cortical brain volume are enlarged as determined from 13 contiguous coronal slices. Morphometric evaluation of wt ($n = 5$) or synRas-TG ($n = 5$) mice was performed by using NMR imaging and a semiautomatic imaging software on a Silicon Graphics Indy computer.

no detectable increase in Ras-TG protein in the cerebellum of synRas-TG mice (Fig. 1 B). A second line (line 46) was investigated and showed comparatively low Ras-TG expression levels in total brain (not shown). Unless otherwise stated, the results derive from using heterozygous line 50 with wt littermates as controls.

LacZ activity was used to detect the presence of the dicistronic transgenic mRNA. Fig. 1 C shows a horizontal section through a lacZ-stained hemisphere of a wt mouse brain at 6 mo old compared with that of a synRas-TG mouse. The cortex of the synRas-TG mouse is clearly enlarged. It is wider in the medio-lateral direction and extends further caudally, covering more of the tectum than the wt cortex. The larger cortex has slightly displaced the cerebellum. Blue-labeled (lacZ-positive) neurons are evident mainly in the cortex and hippocampus. Cellular analysis of lacZ activity indicated that the Ras-TG expression was always restricted to neurons. The latter were distinguished from glia cells by smooth, rounded nuclei with a large clear nucleolus. Ras-TG expression was detected in the claustrum and amygdala, and neuronal subsets in the olfactory bulb, septum, Broca band, preoptic area, anterior and midline thalamic nuclei, tegmentum including substantia nigra, but not in sensory thalmic nuclei (ventrobasal complex and geniculate nuclei) or the tectum (data not shown).

To quantify in vivo the increase in brain volume seen in the fixed slices, a morphometric evaluation was performed by NMR imaging using slices of 1-mm thickness (Fig. 1 D). The volume of the intact cortex increased by 12.7% from 145.2 ± 3.4 µl to 163.6 ± 3.8 µl ($n = 5$, $P < 0.01$), and the total brain volume increased by 14.5% from 388.7 ± 5.7 µl to 444.1 ± 20.6 µl ($n = 5$, $P < 0.05$), respectively. Brain volume expansion in synRas-TG mice could have arisen from increased neuronal cell numbers or hypertrophy of individual neurons. Therefore, we determined the neuronal cell numbers in the cortex of synRas-TG mice by applying the dissectors method to serial semithin sections of five randomly located samples of the frontal, parietal, and occipital cortex (Sterio, 1984). The number of cortical neurons remained unchanged (wt, $6.942 \pm 0.782 \times 10^6$, $n = 5$; synRas TG, $7.077 \pm 0.782 \times 10^6$, $n = 5$), resulting in a decreased numerical density from 80.3 ± 6.32 ($\times 10^3$

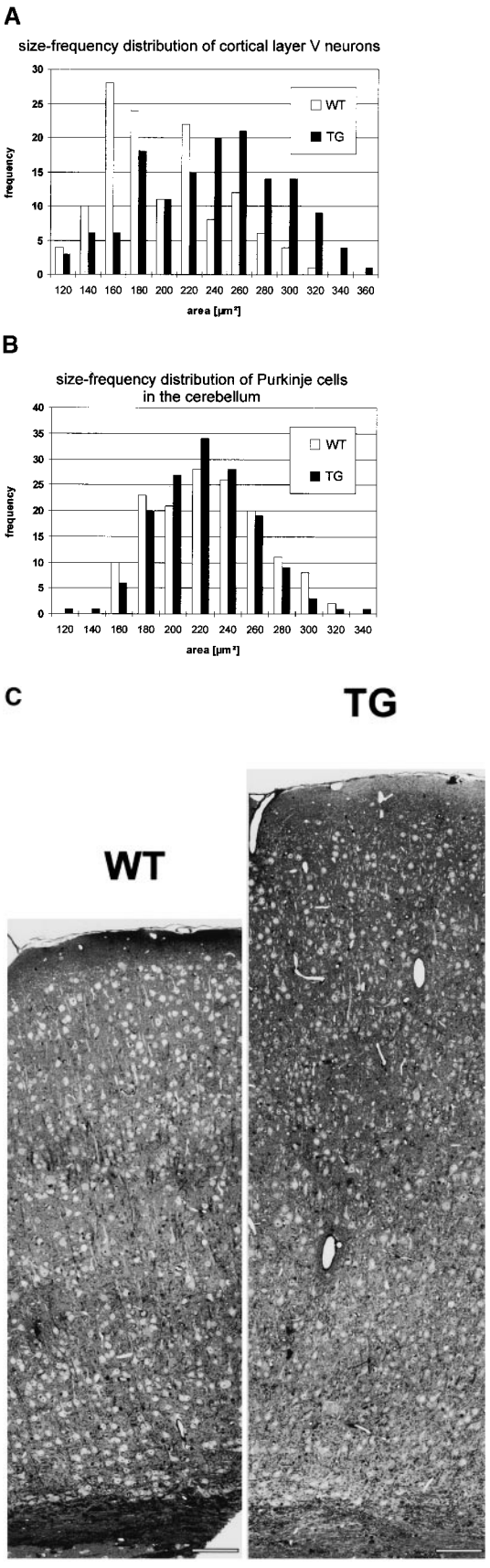

Figure 2. (A) Size-frequency distributions of cortical, hippocampal, and cerebellar neurons. Size-frequency distribution of large pyramidal neurons of layer V in the motor and somatosensory cortex. Note the shift to larger areas, giving rise to new large diameter size classes. (B) Size-frequency distribution of Purkinje cells of the cerebellum. No changes in Purkinje cell soma sizes are observed. (C) Cross-section through the parietal cortex demonstrating the expansion of the cortical size in synRas-TG mice. Bars, 100 μm.

mm^{-3} in wt) to 66.74 ± 5.76 ($\times 10^3$ mm^{-3}, $P < 0.05$) in synRas-TG.

Brain Region–Specific Expansion of Neuronal Cell Soma Diameter

The size-frequency histogram of cross-sectional areas of the layer V pyramidal neurons in the motor and somatosensory cortex showed a significant shift to larger soma areas, including size classes above the normal range at 6 mo old animals ($P \leq 0.0001$) (Fig. 2 A). This neuronal hypertrophy was developmentally regulated, corresponding to the neuronal Ras-TG expression levels. At P4, changes were barely detectable, i.e., differences were not significant, whereas, at P13, the increases in soma areas were highly significant ($P \leq 0.0001$) (data not shown). Neuronal hypertrophy and cortical expansion were most prominent in the frontal or parietal cortex (Fig. 2 C). In the cerebellum, the cross-sectional areas of the individual Purkinje neurons were not changed in their size distribution (Fig. 2 B).

Significant ($P \leq 0.0001$) increases in cortical soma area in layer V pyramidal neurons was also found in line 46 at 6 mo old.

Constitutive Activation of Ras and MAPKs (ERK1 and ERK2), but Not PI 3-kinase and Akt/PKB

To test whether the Ras-TG protein was active in neurons, we captured active GTP-Ras selectively with a peptide derived from Raf kinase (de Rooij and Bos, 1997). A major Ras activity was found in extracts of the hippocampus and cortex, but only low levels were detected in the cerebellum of synRas-TG mice. In wt littermates, the basal activity of endogenous Ras was hardly detectable under these experimental conditions (Fig. 3, second row). Because chronic treatment of responsive PC12 cells with NGF increases synapsin I synthesis (Romano et al., 1987), we tested if neuronal Ras-TG activity regulates endogenous synapsin levels in the brain. Fig. 3 A shows that the synapsin levels were not different between synRas-TG mice and wt littermates in all regions investigated. Moreover, the Ras-TG expression pattern reflected the endogeneous synapsin promoter activity, with low expression in the cerebellum and high levels in hippocampus or cortex, indicating that Ras-TG activity does not regulate the endogeneous *synapsin I* promoter.

As expected from the increased Ras activities in synRas-TG mice, phosphorylation of MAPKs (ERK-1 and/or ERK-2) was constitutively elevated in all three brain regions without any changes in MAPK protein expression (Fig. 3 A). The differential increase in phosphorylation of ERK-1 or ERK-2 was especially pronounced in the hippocampus and cortex where mainly ERK 1 was activated in all cases tested ($n = 3$).

Besides the MAPK pathway, Ras activates the catalytic subunit of PI 3-kinase subtypes as a downstream target

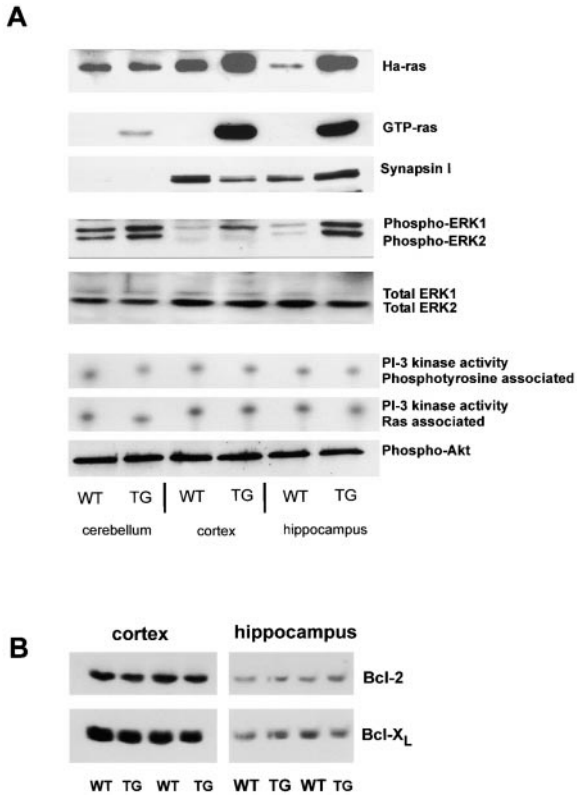

Figure 3. Effects of neuronal Ras-TG expression on major signal transduction pathways. (A) Ha-Ras expression: crude brain lysates were separated by SDS-PAGE and blotted on nitrocellulose. Ha-Ras expression was detected with a Ha-Ras–specific antibody. Note the increased levels of Ha-Ras protein in cortical and hippocampal brain lysates (synRas-TG). No overexpression of Ha-Ras was found in the cerebellum of synRas-TG mice. GTP-Ras levels: GTP-Ras was precipitated from crude lysates using glutathione–Sepharose loaded with a fusion protein consisting of glutathione-*S*-transferase and the Ras-binding domain of Raf. The affinity precipitates were separated by SDS-PAGE and blotted on nitrocellulose. The amount of signaling active GTP-bound conformation of Ras proteins was detected using a pan-Ras antibody. Transgenic V12-Ha-Ras expression results in a major increase of GTP-Ras in the cortex and hippocampus, but only an attenuated increase is observed in the cerebellum. Endogenous synapsin I expression: in adult cerebellum, the relative levels of Synapsin expression are low compared with cortex and hippocampus. Note that the Ras activity in synRas-TG mice does not regulate the endogenous Synapsin levels. MAPK phosphorylation: crude brain lysates were separated by SDS-PAGE, blotted on nitrocellulose, and MAPK phosphorylation was detected using an antibody specific for MAPK (ERK1 and ERK2) phosphorylated on the activation-competent threonine and tyrosine. In synRas-TG mice, MAPK tyrosine phosphorylation in neurons is permanently enhanced, though protein levels (ERK1 and ERK2) are not affected (see below). MAPK phosphorylation is enhanced most prominently in the hippocampus, but only moderately in the cerebellum, thus, corresponding to the different synRas-TG expression levels. In the cortex, we observe a more selective ERK1 over ERK2 phosphorylation. MAPK—total protein content: equal amounts of protein were loaded in each slot, resulting in similar signals for total amounts of ERK1 or ERK2. PI 3-kinase activity: the levels of phosphatidylinositol 3-phosphate (PI[3]P) reaction products were determined in coimmunoprecipitates using either anti-pTyr antibodies or anti-Ras monoclonal antibody 13-259. Neither the phosphotyrosine-associated, nor the Ras-associated, PI 3-kinase activity was altered. Akt (PKB) phosphorylation: crude brain lysates were separated by SDS-PAGE, blotted on nitrocellulose, and phosphorylation of the PI 3-kinase target Akt was detected using an antibody specific for Akt phosphorylated on serine 473. The phosphorylation of Akt is not altered by the Ras-TG activity in neurons. (B) Levels of Bcl-2 and Bcl-X_L are not altered by the Ras-TG activity in Western blots, as determined by antibodies to Bcl-2 or Bcl-X_L.

(Rodriguez-Viciana et al., 1996; Walker et al., 1999). However, PI 3-kinase activity remained unchanged in brain homogenates of wt compared with synRas-TG littermates. Consistently, the levels of phosphorylations of the PI 3-kinase target, Akt-1/PKB (Franke et al., 1995), also remained unchanged (Fig. 3 A, bottom row). Since Bcl-2 or Bcl-X_L have been previously shown to be regulated by neurotrophins and MAPKs (Liu et al., 1999), their respective protein levels were investigated. These remained unchanged in synRas-TG mice in cortex and hippocampus, regions of high transgene expression (Fig. 3 B).

Enhanced Chat or TH Activities and Increased Neuropeptide Y Expression

Besides induction of neuronal hypertrophy, neurotrophic actions include the regulation of neurotransmitter synthesizing enzymes, such as Chat or TH. Specific Chat activity in homogenates containing the septal region from the basal forebrain of synRas-TG mice was 89% higher than in homogenates of wt littermates (942 ± 181 pmol/mg/min, $n = 6$ versus 498 ± 149 pmol/mg/min, $n = 9$, $P < 0{,}001$). TH activity was elevated by 30.6 ± 31% ($n = 5$, $P < 0.05$) in the mesencephalic forebrain region containing the dopaminergic neurons of the substantia nigra.

Next, we asked if the activated Ras-TG also affects the neurochemical properties of cortical inhibitory interneurons known to express TrkB-receptors (Gorba and Wahle, 1999). Fig. 4 shows that the staining intensity and the density of cortical NPY-expressing neurons clearly increased throughout the cortex, despite cortical expansion (from 54 to 80 cells/mm^2 in sagital sections, $P \leq 0.01$). In contrast to neocortex, NPY mRNA expression appeared to remain identical in hilus interneurons in the hippocampus and in neostriatal interneurons (not shown). The staining intensity and density of GAD (Fig. 4) or parvalbumin mRNAs (not shown) were not affected.

The motorneurons of the facial nucleus were investigated in more detail. In situ lacZ–mRNA hybridization revealed that in the facial nucleus region the typical large diameter motorneurons were clearly lacZ positive (Fig. 5 A). No positive glial cells were found throughout the brain (not shown). As a functional consequence of the Ras-TG expression, we found a 25.6% ($P < 0.001$, $n = 100$) increase in the cross-sectional area of the motorneuron somata (Fig. 5 B). Similarly, in the weak Ras-TG–expressing mouse line 46, an attenuated, yet significant, increase in cross-sectional area of the motorneuron somata was found ($P < 0.005$, $n = 143$, data not shown). Finally, we investigated if the Ras-TG activity might regulate the basal activity of Chat in motorneurons, as it was found in the septum. The Chat activity per facial nucleus was indeed elevated by 39% ($n = 3$) (Fig. 5 B, insert), suggesting an increased Chat activity per motorneuron, because their number remained unchanged in the synRas-TG mice.

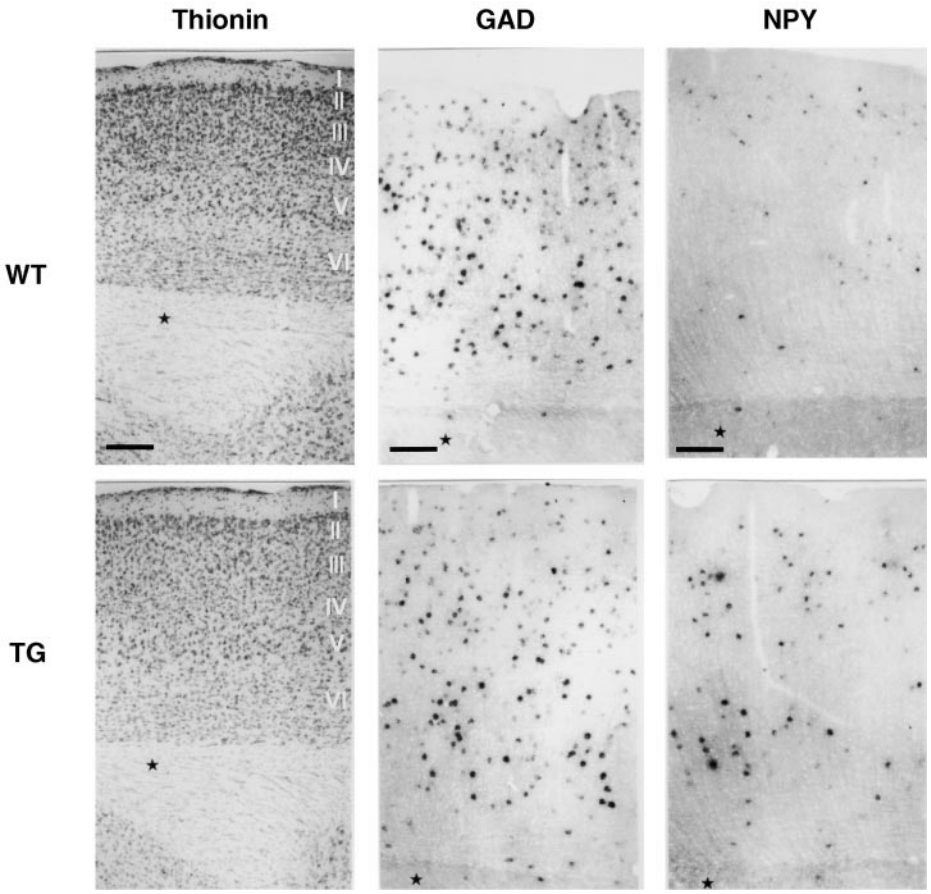

Figure 4. In situ mRNA determination of cDNAs coding for NPY and GAD. Thionin staining (Thionin) of a cross-section through the cortex with layers I–VI is shown, as indicated for wt (top) or synRas-TG (bottom) mice. Bar, 150 μm. The density and intensity of NPY mRNA–expressing neurons is upregulated throughout the cortex of synRas-TG mice (NPY, top and bottom). Bar, 100 μm. However, GAD cDNA expression is not affected (GAD, top and bottom). Bar, 100 μm. Note the increased cross-sectional length of the total cortical layer from the pia mater to the borderline layer VI between wt (~720 μm) and synRas-TG mice (compare stars).

Ras-TG Expression in Motorneurons of the Facial Nucleus Completely Prevents Their Degeneration after Nerve Lesion

To test whether the Ras activation not only prevents embryonic apoptosis (see Introduction), but also promotes protection against lesion-induced neuronal degeneration, we performed facial nerve lesions in young-adult mice (10 wk old). There was on average a 34% reduction in cell number of wt mice, whereas there was no reduction (3%, not significant) in the synRas-TG littermates, as shown by counting the number of nucleoli-containing neurons in every third section of the facial nuclei from five mice each (Fig. 6, B and C). Morphologically, neurons appeared healthy on the lesioned side, with no signs of degeneration or shrinkage in synRas-TG mice (Fig. 6 A).

Ras-TG Expression Attenuates Neurotoxic Insults by 6-OHDA, MPP^+, and MPTP in the Substantia Nigra

We next investigated whether the Ras-TG was expressed in the dopaminergic neurons of the substantia nigra of the synRas-TG mice. Fig. 7 A shows an example of a TH-expressing neuron of the substantia nigra that was Ras-TG–positive. We then asked if the Ras-TG expression could induce protective mechanisms against the neuronal-type–specific toxins 6-OHDA or MPP^+ (Lotharius et al., 1999). Mesencephalic embryonic cultures containing TH-positive neurons were established and neurons were allowed to mature for a period of 5 d. Treatment with 6-OHDA for 90 min or MPP^+ exposure for 36 h reduced the number of TH-positive neurons to 36 or 25% of untreated controls, respectively. In cultures of synRas-TG mice, the loss was partially prevented resulting in a 48 or 34% enhancement of survival after 6-OHDA or MPP^+ treatment (Fig. 7 B).

We also tested the striatal projection area of dopaminergic substantia nigra neurons. In unlesioned animals, there was a 22% increased level of dopamine in synRas-TG mice compared with wt littermates (Fig. 7 C). After two consecutive applications of MPTP, dopamine levels were reduced from 10336 ± 1489 ng/g (n = 10) to 4029 ± 335 ng/g (n = 8) in wt and from 12599 ± 1461 ng/g (n = 11) to 7459 ± 1572 ng/g (n = 8) in synRas-TG mice, thus indicating a subtantial protection.

Discussion

To investigate the physiological role of the proto-oncogene Ras in the adult mammalian nervous system, constitutively activated V12-Ha-Ras was expressed postnatally in the brain of transgenic mice. By using the synapsin I promoter, expression of the Ras-TG was restricted to neurons, giving rise to healthy transgenic mice with a normal life span.

In the synRas-TG mice, we observed pronounced neuronal hypertrophy, one of the earliest described neurotrophic effects in embryonic chick dorsal root ganglion neurons and in sympathetic neurons (Levi-Montalcini, 1987). This hypertrophy was present in several populations of Ras-TG–expressing neurons, i.e., in pyramidal cells of the cortex and in N7 motorneurons of the nucleus facialis. Because the Ras oncogene promotes tumors in cell cycle–

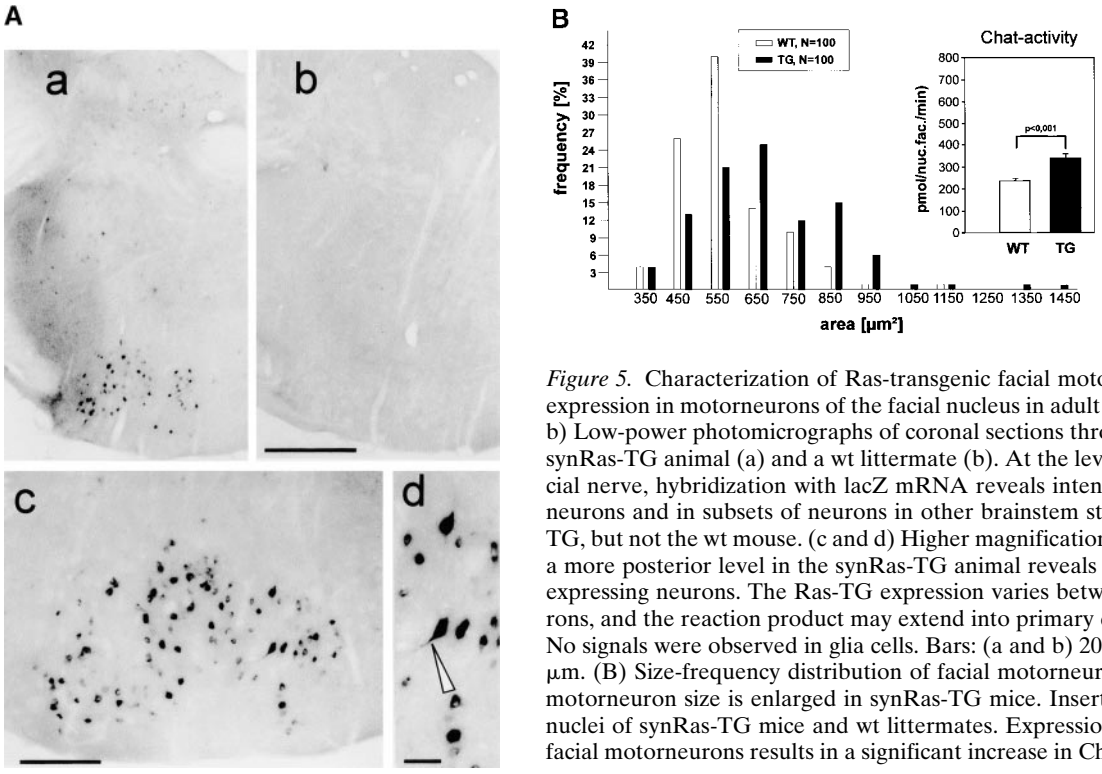

Figure 5. Characterization of Ras-transgenic facial motorneurons. (A) Ras-TG expression in motorneurons of the facial nucleus in adult mice (6 mo old). (a and b) Low-power photomicrographs of coronal sections through the brainstem of a synRas-TG animal (a) and a wt littermate (b). At the level of the genu of the facial nerve, hybridization with lacZ mRNA reveals intense signals in N7 motorneurons and in subsets of neurons in other brainstem structures in the synRas-TG, but not the wt mouse. (c and d) Higher magnification of the facial nucleus at a more posterior level in the synRas-TG animal reveals intensely lacZ mRNA–expressing neurons. The Ras-TG expression varies between the individual neurons, and the reaction product may extend into primary dendrites (arrow head). No signals were observed in glia cells. Bars: (a and b) 200 μm; (c) 50 μm; (d) 20 μm. (B) Size-frequency distribution of facial motorneurons. The average facial motorneuron size is enlarged in synRas-TG mice. Insert: Chat activity in facial nuclei of synRas-TG mice and wt littermates. Expression of Ras-TG protein in facial motorneurons results in a significant increase in Chat activity.

competent cells of transgenic mice (Sinn et al., 1987; Chin et al., 1999), an effect on brain cell number of synRas-TG mice could not be excluded. However, we found that—especially in frontal and parietal cortical regions—neuronal density was decreased, but neuronal numbers were unchanged. This suggests that Ras-TG expression occurred at functionally relevant levels only in fully differentiated neurons whose numbers were not determined by precursor cell division or developmentally regulated cell death. Increased brain size due to cellular hypertrophy (megencephaly) has also been described in a spontaneous mouse mutant (Donahue et al., 1996). Furthermore, in humans, unilateral megencephaly (hemimegalencephaly) occurs as an uncommon sporadic nonfamilial congenital dysplastic abnormality of the central nervous system, but the mechanisms of neuronal cell size regulation are not known (Bosman et al., 1996). Interestingly, in wing cells of *Drosophila*, Ras activity has been shown to promote hypertrophy that is mediated in part by enhanced expression of *dmyc* (Prober and Edgar, 2000).

Our finding that activities of neurotransmitter-synthesizing enzymes regulated by neurotrophic factors, such as Chat activity of the septal or nucleus facialis regions (Gnahn et al., 1983) and the TH activity of the substantia nigra (Hagg, 1998), are increased in synRas-TG mice fits with the notion that Ras activation in neurons could mimic neurotrophic actions. Similarly, brain-derived neurotrophic factor stimulates NPY synthesis, and, during development, NPY mRNA is transiently increased in cortical interneurons, reaching maximal levels at ~30 d postnatally and is then downregulated (Obst and Wahle, 1995). The same developmental profile is displayed by organotypic thalamocortical cocultures. An early "postnatal" application of NT4/5 prevents the developmental downregulation (Wahle et al., 2000). Moreover, blocking spontaneous electrical activity also downregulates NPY mRNA (Wirth et al., 1998). Thus, Ras could mimic neuronal activity, resulting in a maintenance of elevated NPY mRNA levels in the neocortex of adult synRas-TG mice. In PC12 cells, such an increase in TrkB-mediated NPY protein expression is sensitive to blockade by the MEK-inhibitor PD98059, suggesting a role of the MAPK signaling pathway (Williams et al., 1998).

MAPKs (ERKs) are phosphorylated after direct binding of Raf kinases to activated Ras. In addition, some subtypes of PI 3-kinase have been shown to be direct effectors of GTP-bound Ras (Rodriguez-Viciana et al., 1996; Rubio et al., 1997), and PI 3-kinase is a preferred effector of the Ha-Ras isotype used in the synRas-TG mice (Yan et al., 1998). Activation of the PI 3-kinase/Akt-1 (PKB) pathway has been shown to phosphorylate and, thereby, inactivate cell death regulatory proteins (Biggs et al., 1999; Brunet et al., 1999). However, in contrast to our recent results on the rapid increase of PI 3-kinase in response to NGF activation in peripheral neurons (Virdee et al., 1999), constitutive activation of Ras did not reveal any changes in PI 3-kinase activity. The levels of the phosphorylation of the downstream kinase PKB/Akt remained equally unaffected in synRas-TG mice. Thus, the phenotype of synRas-TG mice appears to be independent of a major PI 3-kinase activation in cerebellum, hippocampus, and cortex. Interestingly, PI 3-kinase–independent neuronal survival pathways have been described recently, suggesting that PI 3-kinase activation may not be the sole mechanism of preventing neuronal cell death (Vogelbaum et al., 1998; Virdee et al., 1999; Williams and Doherty, 1999).

One of the major motivations to establish this synRas-TG mouse model was to investigate the possible role of Ras activity in lesion-induced degeneration of the adult nervous system. It has been shown previously that in cul-

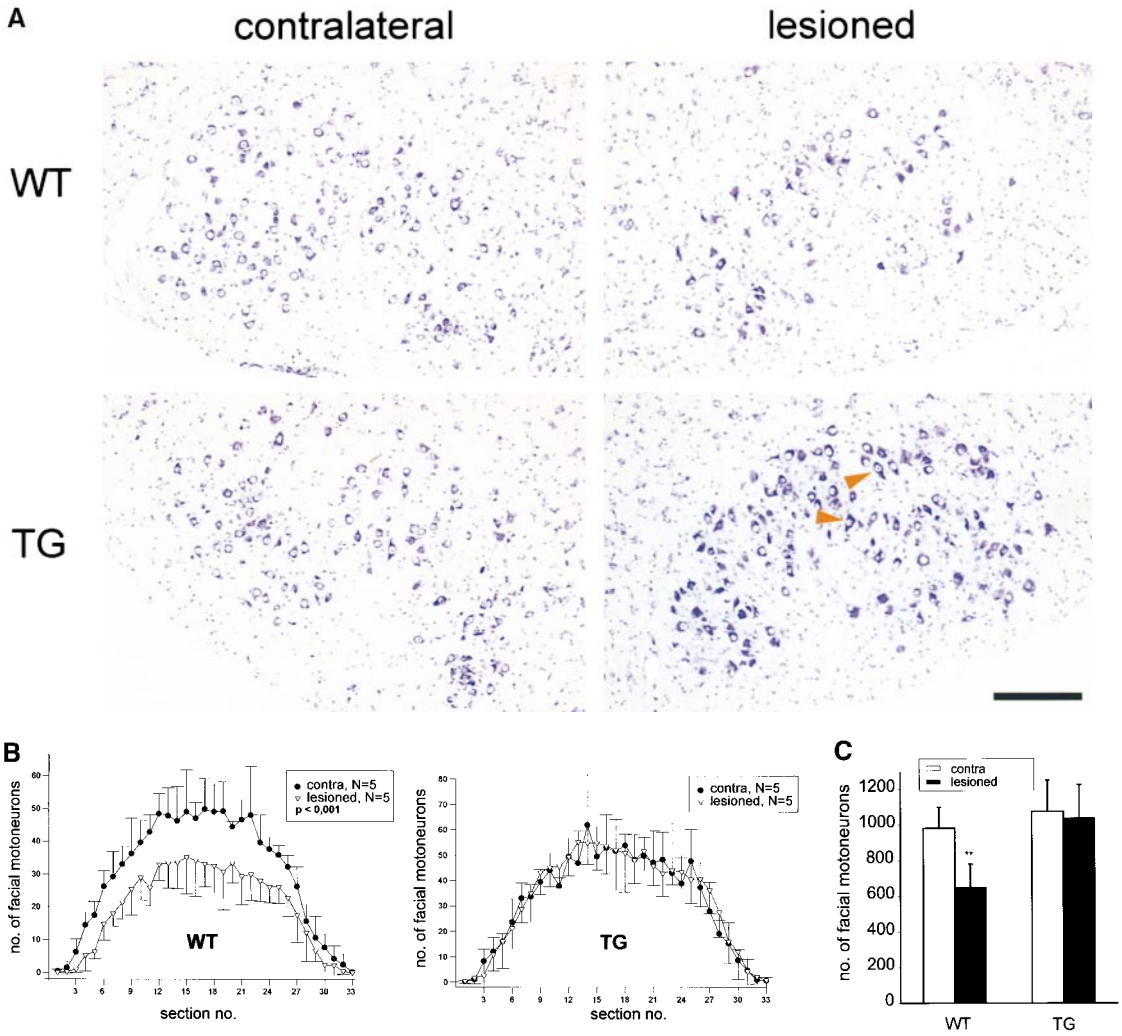

Figure 6. Protection of facial motorneurons from axotomy-induced degeneration. (A) Representative Nissl-stained sections of axotomized mice. The ipsilateral section of the wt mouse shows loss of facial motorneurons compared with the contralateral section, whereas the facial motorneuron number of the synRas-TG mouse remains equal on both sides. Arrowheads indicate well-preserved motorneurons with nucleoli in lesioned synRas-TG mice. Bar, 50 μm. (B) The number of facial motorneurons per section. Facial motorneurons of one out of three sections were counted. The first section is determined by the appearance of the first counted facial motorneuron. For better visualization, the ipsilateral distribution curve was centered within the contralateral distribution curve. Determination of wt facial motorneuron numbers reveals severe axotomy-induced degeneration along the total ipsilateral nucleus length, which cannot be detected in the synRas-TG mice. (C) The number of counted facial motorneurons per nucleus. Facial motorneurons of one out of three sections were counted. Total numbers of facial motorneurons per nucleus were not extrapolated. Analysis of counted facial motorneuron numbers reveals full protection of facial motorneurons from axotomy-induced degeneration by the transgene.

tures of embryonic neurons ligand-independend survival is achieved by intracellular application of activated Ras in chick dorsal root ganglia neurons, in superior cervical ganglion neurons, or in spinal motorneurons (Borasio et al., 1989; Nobes et al., 1996; Weng et al., 1996; Mazzoni et al., 1999). Our finding that constitutively activated Ras in neurons completely prevented axotomy-induced degeneration of adult facial motorneurons shows that the activation of the Ras pathway promotes protective functions in vivo.

Survival of motorneurons is also enhanced by expression of Bcl-2 in transgenic mice and in *Bax* knock out mice because axotomy-induced motorneuron death was prevented (Martinou et al., 1994; Deckwerth et al., 1996). In our system, considering the lack of changes in levels of Bcl-2 or Bcl-X_L, together with the lack of activation of PKB/Akt, we assume that an as yet unidentified downstream target of Ras, other than the Bcl-2 family of proteins, may be involved in the Ras-mediated neuronal rescue.

In addition to motorneurons, dopaminergic neurons of the substantia nigra were investigated, because they serve as a model of neurons affected in Parkinson's disease. 6-OHDA and MPP^+ were used as toxins that are thought to be specific for neurons carrying the dopamine transporter. Although the mechanism by which MPP^+ causes neuronal degeneration appears to be distinctly different (Lotharius et al., 1999), the adverse effects of both types of toxins could be attenuated in dopaminergic neurons of synRas-TG mice. Interestingly, suppression of Ras activity in PC12 cells rendered them more sensitive to toxic radicals (Guyton et al., 1996), and, similarly, in rat sympathetic neurons, NGF-induced suppression of radical formation was dependent on the concommittent activation of MAPK (Dugan et al., 1997).

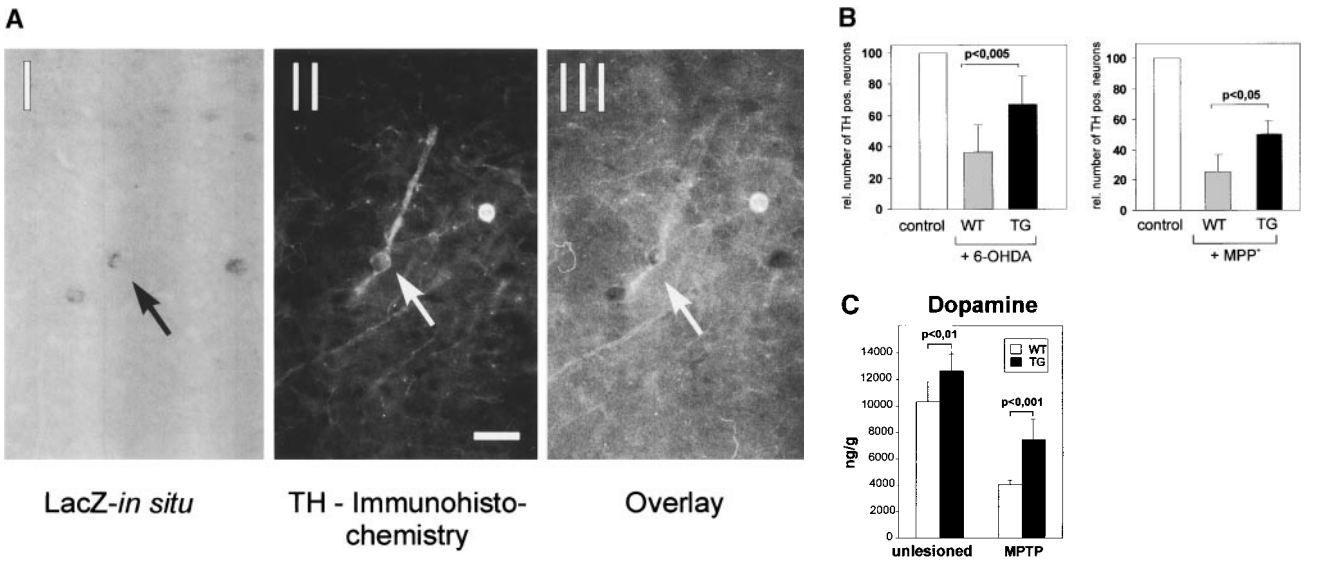

Figure 7. Characterization of transgenic midbrain dopaminergic neurons and protection against neurotoxin-induced degeneration. (A) Expression of the Ras-TG in dopaminergic neurons of the substantia nigra. (I) A coronal section through the midbrain at the level of the substantia nigra was hybridized with a lacZ riboprobe and showed staining in a subset of neurons. (II) Immunohistochemical analysis of the same section using a monoclonal antibody against TH (Roche) and a Texas red–labeled secondary antibody shows TH expression in the neuron expressing the transgene. Bar, 20 μm. (III) Overlay of the immunofluorescence picture and the brightfield micrograph, indicating that the Ras-TG transcript is found in the TH-positive neuron. (B) Effect of 6-OHDA or MPP^+ treatment on the number of cultured midbrain dopaminergic neurons derived from synRas-TG mice or their wt siblings. Midbrain dopaminergic neurons were derived from E14 embryos and cultured under serum-free conditions. After treatment with MPP^+ (1 μM) for 36 h or 6-OHDA (150 μM) for 90 min, cells were fixed with methanol. Dopaminergic neurons were identified using a monoclonal antibody against TH (Roche), a biotin-labeled secondary antibody (Sigma-Aldrich), and a streptavidine–FITC conjugate. After counting dopaminergic neurons, the genotype was determined by Southern blot analysis. Treatment with the toxin resulted in degeneration of the dopaminergic neurons. This toxin-induced degeneration was markedly reduced in cultures derived from synRas-TG mice. The numbers of non-dopaminergic neurons remained unchanged (data not shown). (C) Determination of dopamine after in vivo treatments with MPTP in synRas-TG mice and their wt siblings (see Materials and Methods). In the synRas-TG mice, the MPTP-induced decrease of dopamine contents was profoundly reduced.

In summary, we present a model of a neuroprotective mechanism promoted by constitutive activation of Ras in adult central nervous system neurons. It is now possible to test if neural stem cells derived from synRas-TG mice can be isolated, cultured, and transplanted to result in stabilized differentiated neurons due to the Ras-TG expression in the adult mouse brain. The success of transplants of dopaminergic embryonic mesencephalic neurons into Parkinson's patients has been shown to depend on the preservation of TH activity of the transplant (Wenning et al., 1997; Piccini et al., 1999), and methods for neuronal stabilization before transplantation are desirable. In addition, pharmacological downregulation of a recently described neuronal-specific NF splice variant (Geist and Gutmann, 1996) could be tested for a possible enhancement of endogenous Ras activity. Thus, investigations on the Ras-mediated neuroprotection in vivo may help to develop new therapeutic strategies against neurodegenerative diseases.

The authors thank Dr. M.W. Kilimann, for his gift of the synapsin I promoter, Dr. Max Holzer for help with neuronal countings, Dr. Kai Erdmann for Western blots, Dr. Janos Peli for DNA injections, Dr. Manfred Eis for magnetic resonance imaging measurements, Dr. Aviva Tolkowsky, Dr. Gian D. Borasio, and Dr. Irmgard Dietzel for critically reading the manuscript, and Dr. Paul Greengard for providing us with the synapsin I antibody. For technical assistance, we are grateful to Mr. Thomas Ferrat, Mr. Kurt Stöcklin, Mrs. Anne-Marthe Buchle, Mr. Willi Theilkäs, and Mrs. Sabine Laerbusch. For animal care and genotyping, we thank Dr. Markus Schröder and Mr. Stefan Jappert.

This work was supported by a Bundesministerium für Bildung, Wissenschaft, und Forschung (BMBF) grant and by the Deutsche Forschungsgemeinschaft (DFG).

Submitted: 19 July 2000
Revised: 19 October 2000
Accepted: 23 October 2000

References

Allegrini, P.R., and D. Sauer. 1992. Application of magnetic resonance imaging to the measurement of neurodegeneration in the rat brain: MRI data correlate strongly with histology and enzymatic analysis. *Magn. Reson. Imaging.* 10:773–778.

Bar-Sagi, D., and J.R. Feramisco. 1985. Microinjection of the ras oncogene protein into PC12 cells induces morphological differentiation. *Cell.* 42:841–848.

Biggs, W.H., J. Meisenhelder, T. Hunter, W.K. Cavenee, and K.C. Arden. 1999. Protein kinase B/Akt-mediated phosphorylation promotes nuclear exclusion of the winged helix transcription factor FKHR1. *Proc. Natl. Acad. Sci. USA.* 96:7421–7426.

Bollag, G., and F. McCormick. 1991. Differential regulation of rasGAP and neurofibromatosis gen product activities. *Nature.* 351:576–579.

Bonni, A., A. Brunet, A.E. West, S.R. Datta, M.A. Takasu, and M.E. Greenberg. 1999. Cell survival promoted by the ras-MAPK signaling pathway by transcription-dependent and -independent mechanisms. *Science.* 286:1358–1362.

Borasio, G.D., J. John, A. Wittinghofer, Y.A. Barde, M. Sendtner, and R. Heumann. 1989. ras p21 protein promotes survival and fiber outgrowth of cultured embryonic neurons. *Neuron.* 2:1087–1096.

Borasio, G.D., A. Markus, A. Wittinghofer, Y.A. Barde, and R. Heumann. 1993. Involvement of ras p21 in neurotrophin-induced response of sensory, but not sympathetic neurons. *J. Cell Biol.* 121:665–672.

Bosman, C., R. Boldrini, L. Dimitri, C. Di Rocco, and A. Corsi. 1996. Hemimegalencephaly. Histological, immunohistochemical, ultrastructural and cytofluorimetric study of six patients. *Childs. Nerv. Syst.* 12:765–775.

Bostwick, J.R., and W.D. Le. 1991. A tyrosine hydroxylase assay in microwells using coupled nonenzymatic decarboxylation of dopa. *Anal. Biochem.* 192: 125–130.

Brambilla, R., N. Gnesutta, L. Minichiello, G. White, A.J. Roylance, C.E. Herron, M. Ramsey, D.P. Wolfer, V. Cestari, C. Rossi-Arnaud, et al. 1997. A role for the Ras signalling pathway in synaptic transmission and long-term memory. *Nature.* 390:281–286.

Brewer, G.J., and C.W. Cotman. 1989. Survival and growth of hippocampal neurons in defined medium at low density: advantages of a sandwich culture technique or low oxygen. *Brain Res.* 494:65–74.

Brunet, A., A. Bonni, M.J. Zigmond, M.Z. Lin, P. Juo, L.S. Hu, M.J. Anderson, K.C. Arden, J. Blenis, and M.E. Greenberg. 1999. Akt promotes cell survival by phosphorylating and inhibiting a Forkhead transcription factor. *Cell.* 96: 857–868.

Capon, D.J., E.Y. Chen, A.D. Levinson, P.H. Seeburg, and D.V. Goeddel. 1983. Complete nucleotide sequences of the T24 human bladder carcinoma oncogene and its normal homologue. *Nature.* 302:33–37.

Chin, L., A. Tam, J. Pomerantz, M. Wong, J. Holash, N. Bardeesy, Q. Shen, R. O'Hagan, J. Pantginis, H. Zhou, et al. 1999. Essential role for oncogenic Ras in tumour maintenance. *Nature.* 400:468–472.

de Rooij, J., and J.L. Bos. 1997. Minimal Ras-binding domain of Raf1 can be used as an activation-specific probe for Ras. *Oncogene.* 14:623–625.

Deckwerth, T.L., J.L. Elliott, C.M. Knudson, E.M.J. Johnson, W.D. Snider, and S.J. Korsmeyer. 1996. BAX is required for neuronal death after trophic factor deprivation and during development. *Neuron.* 17:401–411.

Donahue, L.R., S.A. Cook, K.R. Johnson, R.T. Bronson, and M.T. Davisson. 1996. Megencephaly: a new mouse mutation on chromosome 6 that causes hypertrophy of the brain. *Mamm. Genome.* 7:871–876.

Dugan, L.L., D.J. Creedon, E.M.J. Johnson, and D.M. Holtzman. 1997. Rapid suppression of free radical formation by nerve growth factor involves the mitogen-activated protein kinase pathway. *Proc. Natl. Acad. Sci. USA.* 94: 4086–4091.

Fonnum, F. 1975. A rapid radiochemical method for the determination of choline acetyltransferase. *J. Neurochem.* 24:407–409.

Franke, T.F., S.I. Yang, T.O. Chan, K. Datta, A. Kazlauskas, D.K. Morrison, D.R. Kaplan, and P.N. Tsichlis. 1995. The protein kinase encoded by the Akt proto-oncogene is a target of the PDGF-activated phosphatidylinositol 3-kinase. *Cell.* 81:727–736.

Geist, R.T., and D.H. Gutmann. 1996. Expression of a developmentally-regulated neuron-specific isoform of the neurofibromatosis 1 (NF1) gene. *Neurosci. Lett.* 211:85–88.

Ghattas, I.R., J.R. Sanes, and J.E. Majors. 1991. The encephalomyocarditis virus internal ribosome entry site allows efficient coexpression of two genes from a recombinant provirus in cultured cells and in embryos. *Mol. Cell Biol.* 11:5848–5859.

Gnahn, H., F. Hefti, R. Heumann, M.E. Schwab, and H. Thoenen. 1983. NGF-mediated increase of choline acetyltransferase (ChAT) in the neonatal rat forebrain: evidence for a physiological role of NGF in the brain? *Brain Res.* 285:45–52.

Gorba, T., and P. Wahle. 1999. Expression of TrkB and TrkC but not BDNF mRNA in neurochemically identified interneurons in rat visual cortex in vivo and in organotypic cultures. *Eur. J. Neurosci.* 11:1179–1190.

Guha, A., M.M. Feldkamp, N. Lau, G. Boss, and A. Pawson. 1997. Proliferation of human malignant astrocytomas is dependent on Ras activation. *Oncogene.* 15:2755–2765.

Guyton, K.Z., Y. Liu, M. Gorospe, Q. Xu, and N.J. Holbrook. 1996. Activation of mitogen-activated protein kinase by H2O2. Role in cell survival following oxidant injury. *J. Biol. Chem.* 271:4138–4142.

Hagg, T. 1998. Neurotrophins prevent death and differentially affect tyrosine hydroxylase of adult rat nigrostriatal neurons in vivo. *Exp. Neurol.* 149:183–192.

Hoesche, C., A. Sauerwald, R.W. Veh, B. Krippl, and M.W. Kilimann. 1993. The 5′-flanking region of the rat synapsin I gene directs neuron-specific and developmentally regulated reporter gene expression in transgenic mice. *J. Biol. Chem.* 268:26494–26502.

Holland, E.C., J. Celestino, C. Dai, L. Schaefer, R.E. Sawaya, and G.N. Fuller. 2000. Combined activation of ras and akt in neural progenitors induces glioblastoma formation in mice. *Nat. Genet.* 25:55–57.

Kalnins, A., K. Otto, U. Ruther, and B. Muller-Hill. 1983. Sequence of the lacZ gene of *Escherichia coli*. *EMBO (Eur. Mol. Biol. Organ.) J.* 2:593–597.

Katz, M.E., and F. McCormick. 1997. Signal transduction from multiple Ras effectors. *Curr. Opin. Genet. Dev.* 7:75–79.

Kennedy, M.B. 1998. Signal transduction molecules at the glutamatergic postsynaptic membrane. *Brain Res. Brain Res. Rev.* 26:243–257.

Kou, S.Y., A.Y. Chiu, and P.H. Patterson. 1995. Differential regulation of motor neuron survival and choline acetyltransferase expression following axotomy. *J. Neurobiol.* 27:561–572.

Levi-Montalcini, R. 1987. The nerve growth factor 35 years later. *Science.* 237: 1154–1162.

Lietz, M., P. Cicchetti, and G. Thiel. 1998. Inverse expression pattern of REST and synapsin I in human neuroblastoma cells. *Biol. Chem.* 379:1301–1304.

Liu, Y.Z., L.M. Boxer, and D.S. Latchman. 1999. Activation of the Bcl-2 promoter by nerve growth factor is mediated by the p42/p44 MAPK cascade. *Nucleic Acids Res.* 27:2086–2090.

Lockyer, P.J., S. Wennstrom, S. Kupzig, K. Venkateswarlu, J. Downward, and P.J. Cullen. 1999. Identification of the ras GTPase-activating protein GAP1(m) as a phosphatidylinositol-3,4,5-triphosphate-binding protein in vivo. *Curr. Biol.* 9:265–268.

Lotharius, J., L.L. Dugan, and K.L. O'Malley. 1999. Distinct mechanisms underlie neurotoxin-mediated cell death in cultured dopaminergic neurons. *J. Neurosci.* 19:1284–1293.

Manabe, T., A. Aiba, A. Yamada, T. Ichise, H. Sakagami, H. Kondo, and M. Katsuki. 2000. Regulation of long-term potentiation by H-Ras through NMDA receptor phosphorylation. *J. Neurosci.* 20:2504–2511.

Markus, A., A. von Holst, H. Rohrer, and R. Heumann. 1997. NGF-mediated survival depends on p21ras in chick sympathetic neurons from the superior cervical but not from lumbosacral ganglia. *Dev. Biol.* 191:306–310.

Marshall, C.J. 1996. Ras effectors. *Curr. Opin. Cell Biol.* 8:197–204.

Martinou, J.C., M. Dubois-Dauphin, J.K. Staple, I. Rodriguez, H. Frankowski, M. Missotten, P. Albertini, D. Talabot, S. Catsicas, and C. Pietra. 1994. Overexpression of BCL-2 in transgenic mice protects neurons from naturally occurring cell death and experimental ischemia. *Neuron.* 13:1017–1030.

Mazzoni, I.E., F.A. Said, R. Aloyz, F.D. Miller, and D. Kaplan. 1999. Ras regulates sympathetic neuron survival by suppressing the p53-mediated cell death pathway. *J. Neurosci.* 19:9716–9727.

Moore, B.D., J.M. Slopis, E.F. Jackson, A.E. De Winter, and N.E. Leeds. 2000. Brain volume in children with neurofibromatosis type 1: relation to neuropsychological status. *Neurology.* 54:914–920.

Nobes, C.D., J.B. Reppas, A. Markus, and A.M. Tolkovsky. 1996. Active p21Ras is sufficient for rescue of NGF-dependent rat sympathetic neurons. *Neuroscience.* 70:1067–1079.

Noda, M., M. Ko, A. Ogura, D.G. Liu, T. Amano, T. Takano, and Y. Ikawa. 1985. Sarcoma viruses carrying ras oncogenes induce differentiation-associated properties in a neuronal cell line. *Nature.* 318:73–75.

Obst, K., and P. Wahle. 1995. Areal differences of NPY mRNA-expressing neurons are established in the late postnatal rat visual cortex in vivo, but not in organotypic cultures. *Eur. J. Neurosci.* 7:2139–2158.

Piccini, P., D.J. Brooks, A. Bjorklund, R.N. Gunn, P.M. Grasby, O. Rimoldi, P. Brundin, P. Hagell, S. Rehncrona, H. Widner, and O. Lindvall. 1999. Dopamine release from nigral transplants visualized in vivo in a Parkinson's patient. *Nat. Neurosci.* 2:1137–1140.

Pimentel, B., C. Sanz, I. Varela-Nieto, U.R. Rapp, F. De Pablo, and E.J. de La Rosa. 2000. c-Raf regulates cell survival and retinal ganglion cell morphogenesis during neurogenesis. *J. Neurosci.* 20:3254–3262.

Prober, D.A., and B.A. Edgar. 2000. Ras1 promotes cellular growth in the *Drosophila* wing. *Cell.* 100:435–446.

Reuther, G.W., and C.J. Der. 2000. The ras branch of small GTPases: ras family members don't fall far from the tree. *Curr. Opin. Cell Biol.* 12:157–165.

Rodriguez-Viciana, P., P.H. Warne, B. Vanhaesebroeck, M.D. Waterfield, and J. Downward. 1996. Activation of phosphoinositide 3-kinase by interaction with Ras and by point mutation. *EMBO (Eur. Mol. Biol. Organ.) J.* 15:2442–2451.

Romano, C., R.A. Nichols, P. Greengard, and L.A. Greene. 1987. Synapsin I in PC12 cells. I. Characterization of the phosphoprotein and effect of chronic NGF treatment. *J. Neurosci.* 7:1294–1299.

Rubio, I., P. Rodriguez-Viciana, J. Downward, and R. Wetzker. 1997. Interaction of Ras with phosphoinositide 3-kinase gamma. *Biochem. J.* 326:891–895.

Sauerwald, A., C. Hoesche, R. Oschwald, and M.W. Kilimann. 1990. The 5′-flanking region of the synapsin I gene. A G+C-rich, TATA- and CAAT-less, phylogenetically conserved sequence with cell type-specific promoter function. *J. Biol. Chem.* 265:14932–14937.

Silva, A.J., P.W. Frankland, Z. Marowitz, E. Friedman, G. Lazlo, D. Cioffi, T. Jacks, and R. Bourtchuladze. 1997. A mouse model for the learning and memory deficits associated with neurofibromatosis type I. *Nat. Genet.* 15: 281–284.

Sinn, E., W. Muller, P. Pattengale, I. Tepler, R. Wallace, and P. Leder. 1987. Coexpression of MMTV/v-Ha-ras and MMTV/c-myc genes in transgenic mice: synergistic action of oncogenes in vivo. *Cell.* 49:465–475.

Sterio, D.C. 1984. The unbiased estimation of number and sizes of arbitrary particles using the disector. *J. Microsc.* 134:127–136.

Sweetser, D.A., R.P. Kapur, G.J. Froelick, K.E. Kafer, and R.D. Palmiter. 1997. Oncogenesis and altered differentiation induced by activated Ras in neuroblasts of transgenic mice. *Oncogene.* 15:2783–2794.

Virdee, K., L. Xue, B.A. Hemmings, C. Goemans, R. Heumann, and A.M. Tolkovsky. 1999. Nerve growth factor-induced PKB/Akt activity is sustained by phosphoinositide 3-kinase dependent and independent signals in sympathetic neurons. *Brain Res.* 837:127–142.

Vogel, K.S., C.I. Brannan, N.A. Jenkins, N.G. Copeland, and L.F. Parada. 1995. Loss of neurofibromin results in neurotrophin-independent survival of embryonic sensory and sympathetic neurons. *Cell.* 82:733–742.

Vogelbaum, M.A., J.X. Tong, and K.M. Rich. 1998. Developmental regulation of apoptosis in dorsal root ganglion neurons. *J. Neurosci.* 18:8928–8935.

Wahle P., T. Gorba, M.J. Wirth, and K. Obst-Pernberg. 2000. Specification of neuropeptide Y phenotype in visual cortical neurons by leukemia inhibitory factor. *Development.* 127:1943–1951.

Waldmeier, P.C., A.M. Buchle, and A.F. Steulet. 1993. Inhibition of catechol-*O*-methyltransferase (COMT) as well as tyrosine and tryptophan hydroxylase by the orally active iron chelator, 1,2-dimethyl-3-hydroxypyridin-4-one (L1, CP20), in rat brain in vivo. *Biochem. Pharmacol.* 45:2417–2424.

Walker, E.H., O. Perisic, C. Ried, L. Stephens, and R.L. Williams. 1999. Structural insights into phosphoinositide 3-kinase catalysis and signalling. *Nature.* 402:313–320.

Weng, G., M.A. Markus, A. Markus, A. Winkler, and G.D. Borasio. 1996. p21ras supports the survival of chick embryonic motor neurones. *Neuroreport.* 7:1077–1081.

Wenning, G.K., P. Odin, P. Morrish, S. Rehncrona, H. Widner, P. Brundin, J.C. Rothwell, R. Brown, B. Gustavii, P. Hagell, et al. 1997. Short- and long-term survival and function of unilateral intrastriatal dopaminergic grafts in Par-

kinson's disease. *Ann. Neurol.* 42:95–107.
Williams, A.G., A.C. Hargreaves, F.J. Gunn-Moore, and J.M. Tavare. 1998. Stimulation of neuropeptide Y gene expression by brain-derived neurotrophic factor requires both the phospholipase Cgamma and Shc binding sites on its receptor, TrkB. *Biochem. J.* 333:505–509.
Williams, E.J., and P. Doherty. 1999. Evidence for and against a pivotal role of PI 3-kinase in a neuronal cell survival pathway. *Mol. Cell Neurosci.* 13:272–280.
Wirth, M.J., K. Obst, and P. Wahle. 1998. NT-4/5 and LIF, but not NT-3 and BDNF, promote NPY mRNA expression in cortical neurons in the absence of spontaneous bioelectrical activity. *Eur. J. Neurosci.* 10:1457–1464.
Wittinghofer, A. 1998. Signal transduction via Ras. *Biol. Chem.* 379:933–937.
Xue, L., J.H. Murray, and A.M. Tolkovsky. 2000. The Ras/phosphatidylinositol 3-kinase and Ras/ERK pathways function as independent survival modules each of which inhibits a distinct apoptotic signaling pathway in sympathetic neurons. *J. Biol. Chem.* 275:8817–8824.
Yan, J., S. Roy, A. Apolloni, A. Lane, and J.F. Hancock. 1998. Ras isoforms vary in their ability to activate Raf-1 and phosphoinositide 3-kinase. *J. Biol. Chem.* 273:24052–24056.